CORE
Metadata, citation and similar papers at core.ac.uk
Provided by CERN Document Server

DESIGN CONSIDERATIONS FOR THE CLIC PRE-DAMPING RINGS

F. Antoniou, NTUA, Athens, Greece, and CERN, Geneva, Switzerland
Y. Papaphilippou, F. Zimmermann, CERN, Geneva, Switzerland

Abstract

The CLIC pre-damping rings (PDR) have to accommodate a large emittance beam, coming in particular from the positron target and reduce its size to low enough values for injection into the main damping rings (DR). The lattice design is based on theoretical minimum emittance (TME) arc cells and long straight sections filled with damping wigglers. Lattice design optimisation considerations are presented with emphasis to the linear optics functions, tunability, chromatic properties and acceptance. A complete phase advance scan of the TME cells is undertaken for reducing the non-linear resonance driving terms and amplitude dependent tunespread and maximizing the ring's dynamic aperture (DA).

INTRODUCTION

The PDR are an essential part of the CLIC injection complex, as they have to digest a 2.86 GeV beam with a large input emittance, especially coming from the positron source [1], to a low enough emittance for injection to the main DR. The required input and output parameters are given in Table 1 [2]. The large size of the input beam in both horizontal and vertical planes, necessitates a large DA, while the large rms momentum spread, of around 1%, requires a large momentum acceptance. The last requirement imposes a low momentum compaction factor and/or large RF voltage. The low emittance and damping times are achieved by the strong focusing in the TME cells and the inclusion of high field damping wigglers in the long straight sections.

In contrast to the DR, the extremely low output emittance is not the crucial parameter for the PDR. The design is driven by the required large momentum acceptance and DA. An analytical solution is being employed to reveal the properties of the TME cells and to chose the optimal parameters. A phase advance scan is then applied, aiming to the minimization of the resonance driving terms and anharmonicities and enlargement of the DA.

The energy of the ring was recently reconsidered, from 2.424 GeV to 2.86 GeV, as this will help eliminating collective effects, including intra-beam scattering, in the DR.

LINEAR LATTICE OPTIMISATION

The PDR is composed of 2 arc sections ($\sim$ 120 m each) and two long straight sections ($\sim$ 85 m each). The arcs are filled with TME cells. The TME condition is achieved if the horizontal dispersion and beta have their minimum in the center of the dipole and are $\beta_{cd} = \frac{L_d}{2\sqrt{15}}$, $\eta_{cd} = \frac{\theta L_d}{24}$,

Table 1: CLIC PDR Injected and Extracted Parameters

Parameters	injected e^-	injected e^+	extracted
Bunch population [10^9]	4.7	6.4	4.5
Bunch length [mm]	1	9	10
Energy Spread [%]	0.07	1.	0.5
Long. emittance [keV.m]	2	257	121
Hor. Norm. emittance [μm]	100	$7{\cdot}10^3$	63
Ver. Norm. emittance [μm]	100	$7{\cdot}10^3$	1.5

where L_d is the length of the bending magnet and $\theta = \frac{L_d}{\rho} = \frac{2\pi}{N_d}$ the bending angle, for N_d bends in the ring. An analytical solution for the quadrupole strengths based on thin lens approximation was derived [3] and the choice of some initial parameters of the design, like number of dipoles and drift lengths, is performed based on this parameterization. The analytical solution for the TME cells creates a multi-parametric space with all the cell properties (drifts, quad strengths, emittance, chromaticities, momentum compaction factor, etc.), from which one can chose to optimize any of the above.

A first design attempt was aiming at a lower momentum compaction factor in order to maximize the momentum acceptance. This lattice, though, showed a rather poor DA. As the large momentum acceptance can be achieved with a larger RF voltage, the present design is concentrated in the DA optimization. In this case, the parameter to be minimized is the chromaticity, in order to lower the required sextupole strengths.

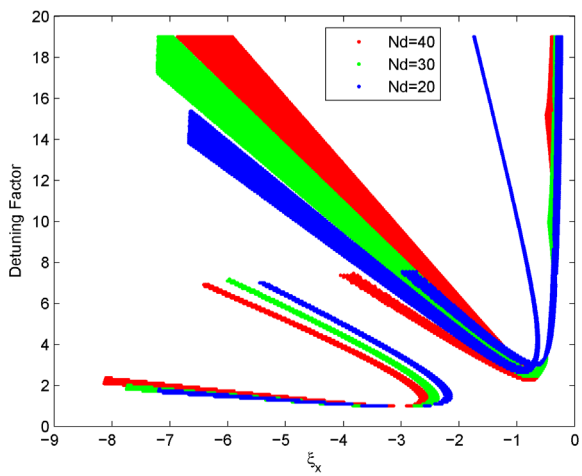

Figure 1: Horizontal chromaticity versus the Detuning Factor for three types of cells.

At first, the optimization of the TME cell is performed by scanning the parameter space of the drifts between the magnetic elements in order to find a cell which is compact enough and provides low chromaticity. The drifts having being fixed, all other optics parameters can be tuned for several values of bending angles θ, and thereby, different values of the achieved minimum emittances. Figure 1 shows the detuning factor, defined as the ratio between the achieved and theoretical minimum emittance, versus the horizontal chromaticity ξ_x. The different colors correspond to different dipole (or cell) numbers. The vertical chromaticity does not have a clear dependence with the detuning factor, as mainly the horizontal optics parameters define the equilibrium emittance. This plot shows that in order to provide the minimum horizontal chromaticity of the cell, a detuning factor > 2 is required. Considering that the minimum number of dipoles necessary to achieve a TME of 50 mm·mrad (the required with a 20% margin) is 20, at least 25 dipoles are needed in order to achieve the same emittance for a detuning factor of 2 while keeping the chromaticity small.

Table 2: Basic Lattice Parameters

Parameters, Symbol [Unit]	Value
Energy, En [GeV]	2.86
Circumference, C [m]	397.4
Bunches per train, N_b	312
Bunch population [10^9]	4.2
Bunch spacing, τ_b [ns]	0.5
Basic cell type	TME
Number of dipoles, N_d	38
Dipole Field, B_a [T]	1.2
Tunes (hor./ver./sync.), (Q_x/Q_y/Q_s)	18.44/12.41/0.07
Nat. chromaticity (hor./vert.), (ξ_x/ξ_y)	-18.99/-22.85
Norm. Hor. Emit., $\gamma\epsilon_0$ [mm·mrad]	47.85
Damping times, (τ_x/τ_y/τ_ϵ) [ms]	2.32/2.32/1.16
Mom. Compaction Factor, α_c [10^{-3}]	3.83
RF Voltage, V_{rf} [MV]	10
RF acceptance, ϵ_{rf} [%]	1
RF frequency, f_{rf} [GHz]	2
Harmonic number, h	2652
Equil. energy spread (rms), σ_δ [%]	0.1
Equil. bunch length (rms), σ_s [mm]	3.27
Number of wigglers, N_{wig}	40
Wiggler peak field, B_w [T]	1.7
Wiggler length, L_{wig} [m]	3
Wiggler period, λ_w [cm]	30

The required damping is mainly achieved by the damping wigglers in the straight sections. The current design uses normal conducting wigglers of 1.7T peak field, 30cm period and total length of 120m, very close to the parameters of PETRA III [5]. The wigglers are placed in FODO cells with phase advances close to 90^o. The optics at the end of the arcs is matched to the straight section with a dispersion suppressor and a matching section. Space is left for injection, extraction and RF cavities. The lattice functions of the TME cell, the wiggler cell, the dispersion suppressor and matching cell and of the whole ring are shown in Fig. 2 and the lattice parameters are displayed in Table 2.

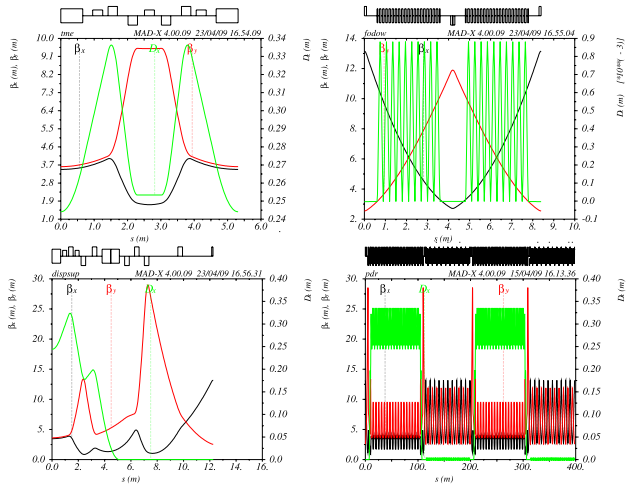

Figure 2: Lattice functions of the TME cell, the wiggler cell, the dispersion suppressor and beta matching cell and of all the ring.

NON LINEAR OPTIMIZATION

The choice of the cell phase advances is crucial for the minimization of the resonance driving terms [4]. It can be demonstrated that a part of a circular machine will not contribute to the excitation of any non-linear resonance, except of those defined by $\eta_x\mu_{x,c} + \eta_y\mu_{y,c} = 2k_3\pi$, if the phase advances per cell satisfy the conditions: $N_c\mu_{x,c} = 2k_1\pi$ and $N_c\mu_{y,c} = 2k_2\pi$, where k_1, k_2 and k_3 are any integers. Prime numbers for N_c, which in our case is the number of TME cells per arc, are interesting because there are less resonances satisfying both diofantine conditions simultaneously. Considering the fact that for the required emittance at least 25 dipoles are needed, convenient numbers of N_c are 11, 13 and 17 which means 26, 30 and 38 dipoles in the ring respectively, including the dispersion suppressors' last dipole. The largest number of cells is better for increasing the detuning factor between the required and the minimum emittance and the cancellation of a larger number of resonance driving terms. Numerical simulations indeed showed that the optimal behavior with respect to non-linear dynamics is achieved for arcs with 17 cells.

A further scanning was performed in both μ_x and μ_y, for values that are integer multiples of 1/17, which minimize the resonance driving terms. Among these, one can choose the phase advances producing the smallest first order tune shift with amplitude in both planes. Figure 3 (top) shows the horizontal versus the vertical phase advance and different colors denote different levels of $\delta q = \sqrt{\delta q_x^2 + \delta q_y^2}$. For some cases, the emittance is also labeled around the respective pair of (μ_x,μ_y). The optimal pair that provides low enough tune shift with amplitude and also the required emittance is $\mu_x = 0.2941 = 5 \cdot \frac{1}{17}$ and $\mu_y = 0.1765 =$

$3 \cdot \frac{1}{17}$. The pair $(0.2941, 0.2352)$ gives also low enough emittance, but smaller DA. Other pairs with smaller horizontal phase advance provide smaller δq, but the emittances are too large. A finer phase advance scan was performed around these values. The results are shown at the bottom of Fig. 3. As before, the different colors show the levels of δq. The tuneshift with amplitude is getting larger as the horizontal phase advance is getting larger, thus the pair of $(\mu_x = 0.2941, \mu_y = 0.1765)$ originally chosen is optimal.

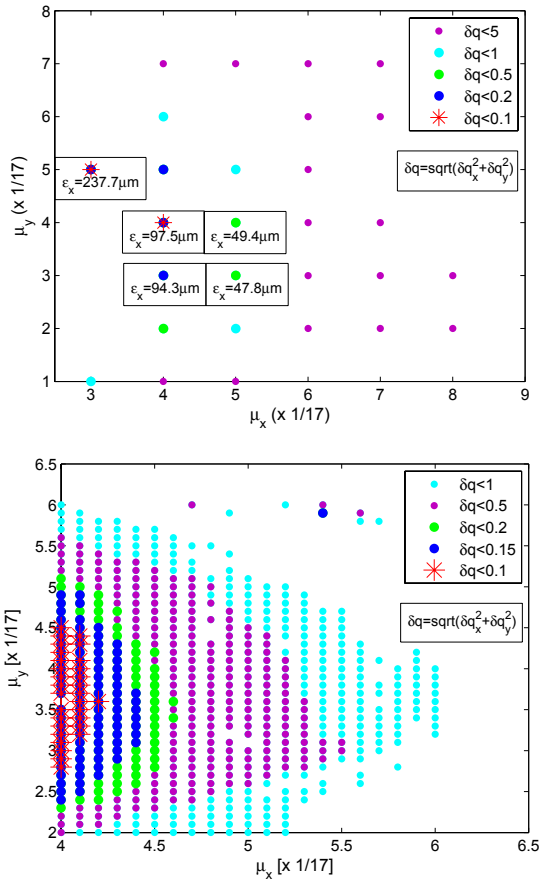

Figure 3: Phase advance scan in integer multiples of 1/17 (top) and a scan around the optimum pair (bottom).

The DA has to be at least larger than the geometric aperture, determined heavily by the large input beam size. At the geometric acceptance limit, a particle has a maximum offset from the design orbit $A = \sqrt{2\beta\epsilon_{edge}} + \eta\delta$ where η the dispersion, δ the momentum deviation and the edge emittance $\epsilon_{edge} = 10\epsilon_{rms}$ [6]. A vertical aperture of $9\sigma_y$ is needed all over the ring, while horizontally, $14\sigma_x$ are needed in the arcs and $9\sigma_x$ in the wiggler section.

The DA of the ring was computed for particles tracked over 1000 turns with MADXPTC [7], and zero, 1% and -1% momentum deviation, neglecting any magnet error effects. The results are shown in Fig. 4. The present design gives an adequate DA which is larger than the geometric aperture. Further improvement can be achieved by the use of harmonic sextupoles. Figure 5 shows the working point in tune space. The on momentum working point is (18.44,12.41) and for large momentum deviations is crossing the forth order (2,-2) resonance, which seems to be the limitation of the off-momentum DA.

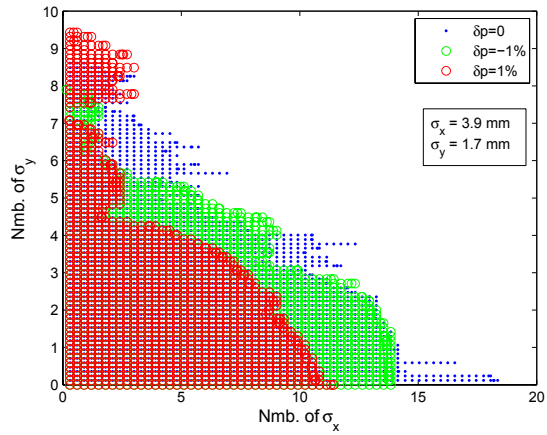

Figure 4: On and off momentum Dynamic Aperture.

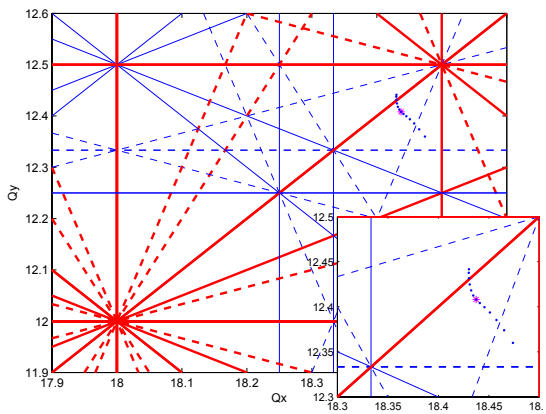

Figure 5: The working point in tune space for momentum deviations from -3% up to 3%. The on-momentum working point is (18.44,12.41).

CONCLUSION

The present design achieves the base line configuration requirements for output parameters and a conformable DA. A working point analysis is in progress. A necessary final step of the non-linear optimization, is the inclusion of non-linear errors in the main magnets and wigglers.

REFERENCES

[1] L. Rinolfi (ed.) et al., WE6RFP065, this conference.
[2] F. Tecker (ed.) et al., CLIC note 764.
[3] F. Antoniou, Y. Papaphilippou, EPAC08, Genova, 2008.
[4] A. Verdier, PAC99, New York, 1999.
[5] M. Tischer et. al., EPAC09, Genoa, 2008.
[6] A. Wolski, LCC-0066, June 2001.
[7] http://mad.web.cern.ch/mad